Vol. 82 (1992) *ACTA PHYSICA POLONICA A* No 2

Proceedings of the ISSSRNS '92, Jaszowiec 1992

XANES EXPERIMENTS FOR HIGH-TEMPERATURE SUPERCONDUCTORS*

A. KOŁODZIEJCZYK

Department of Solid State Physics, Faculty of Physics and Nuclear Technique
University of Mining and Metallurgy, 30-059 Kraków, Poland

The paper presents the results of XANES (X-ray Absorption Near Edge Structure) experiments, of the high-temperature superconductors of Y–Ba–Cu–O-type carried out at the Cu $L_{II,III}$- and O K_I-edges using synchrotron radiation and the KMC double monochromator and SX-700 grading monochromator beamlines of BESSY/Berlin synchrotron storage ring. The aim of the paper is to show that the XANES studies are well suited for characterization of the local electronic structure of the high-temperature superconductors.

PACS numbers: 74.70.–b, 76.30.–v

1. Introduction

The application of synchrotron radiation (SR) in the X-ray spectroscopy (XRS) has resulted in considerable development of experimental information on the electronic structure of atoms, molecules and condensed matter.

This paper contains an introductory part on the X-ray absorption near edge structure, i.e. XANES in the X-ray absorption (XRA) spectrum using SR. Then the analysis of XANES of the high-temperature superconductors (HTS) of Y–Ba–Cu–O-type is presented as an example.

The XANES covers the range of XRA spectrum from the absorption threshold to the energy at which the extended X-ray absorption fine structure (EXAFS) appears.

The SR is specially usefull to carry out XANES experiment because it requires rather high intensity of X-ray phonon flux and high energy resolution of XRA spectra.

Special detection method is used for XANES. Usually, the XRA spectrum is measured by recording the intensity of emitted photoelectrons and Auger electrons or of X-ray fluorescence emission instead of measuring directly the transmitted X-ray intensity. These methods are called the total yield electron mode (TYE) and

*This work was financially supported by the Polish Committee of Scientific Research.

the fluorescent yield mode, respectively. These are used to maximize sensitivity of the XRA spectrum to bulk electronic properties over the surface ones.

In the last paragraph of the paper, as examples, the XANES experiments for the HTS close to the Cu $L_{II,III}$ and O K_I-absorption edges will be presented and comprehensively analysed. This has been carried out making use of SR from the storage ring BESSY/Berlin by the TYE technique. It has turned out to be the powerfull tool to study the local electronic states of copper and oxygen in HTS.

2. General XANES characterisation

In the interaction of X-ray with atoms in the low X-ray photon energy region, say below 10 keV, the main effect is the photoionization process, where a photon is absorbed and an electron is excited. Thus, the XRA spectra in the soft to intermediate X-ray photon energy originate from the excitation of inner-shell electrons of the absorbing atoms with consequent sharp steps in the absorption cross section as the X-ray energy is increased through an inner-shell ionization threshold. Two different regions of the XRA spectrum may be distinguished [1]:

a) near the inner-shell absorption threshold, the so-called "pre-edge and edge region", when the photon energy reaches the given inner-shell state energy or slightly higher energy, and

b) above "ionization threshold" or "continuum threshold", when the photon energy is large enough to eject the inner-shell electron in the continuum, that is the vacuum level in atoms and molecules, the Fermi level in metals, and the bottom of conduction band in insulators.

One observes the pronounced maxima and oscillations in the continuum part of XRA spectra of condensed materials above the photoionization threshold. When the photoelectron energy is about a few electronvolts larger than the photoionization threshold then we are dealing with low kinetic energy photoelectrons which are strongly backscattered by several neighboring atoms, generating multiple-scattering processes [2, 3]. Then the usually strong and sharp features of XRA spectrum over the continuum background just above the absorption threshold are called XANES. For higher energy of X-ray photons the excited photoelectrons possess high kinetic energy and they are only weak scattered by mostly single neighboring atom. Resulting from the single weak scattering process weak oscillations in the XRA spectrum are called EXAFS (extended X-ray absorption fine structure). They are interpreted within more simple single-scattering theory [3, 4] as interference of the reflected electron wave with the outgoing photoelectron waves. It means that one may normally thinks of the XANES extending of the order of 50 eV above the photoionization threshold. This is schematically shown in Fig. 1.

One can distinguish three parts in a XRA spectrum:

1. low energy XANES region, ("threshold region", "pre- and edge region"), over about 10 eV above the photoionization threshold,
2. XANES region up to 50 eV above the photoionization threshold, and
3. EXAFS region above 50 eV to about 200 eV.

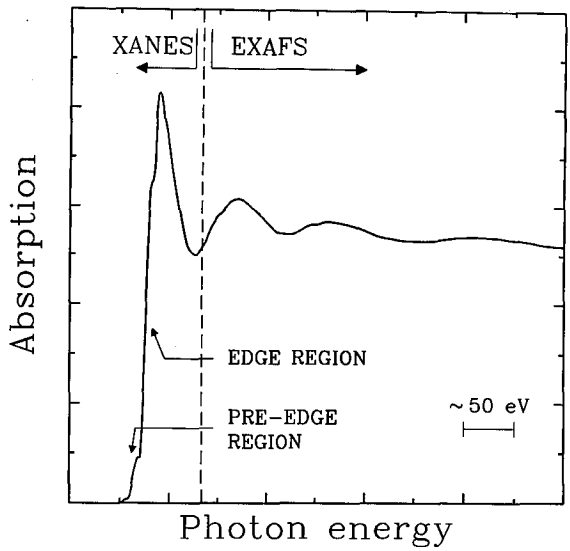

Fig. 1. Schematic of X-ray absorption spectrum showing the threshold region, (including pre-edge and edge regions, i.e. low XANES region), the XANES and the EXAFS regions.

The whole XANES region contains information about the binding energies, quantum numbers, and multiplicities of low-lying bound electronic excited states of the ionized absorbing atom and of low-lying resonant electronic states in the continuum of the absorbing atom, i.e. bound valence states or unoccupied local electronic states in metals and insulators [5]. In other words, the XANES in atoms, molecules, complex ions and biological systems is sensitive to the chemical valency of the absorbing atom and to the coordination geometry and bond angles around the absorbing atom. But in metallic materials the XANES is sensitive to the state populated by the excited photoelectrons which are low-lying extended states bonding the system together and determining its electronic structure and properties. These are all the unoccupied states from the Fermi level up to the EXAFS limit [2]. This includes the unoccupied part of the narrow d bands just above the Fermi level if the XANES of Cu $L_{II,III}$-edges is recorded, as well as the less tightly bound s and p bands for the XANES of O K_I-edge of HTS.

3. Experimental aspects and results

The XANES experiment needs high intensity of X-ray photon flux and high energy resolution of instrumentation for XRA measurements because the one-electron excitations from an inner-core level are always superimposed on the continuum of electronic transitions from the levels with smaller energy. The application of broad-band, highly collimated, intense photon beam from electron storage rings is perfectly suitable to carry out XANES and the conventional X-ray tube laboratory facilities of XRS cannot compete so far in terms of the intensity

and energy resolution with SR. Moreover, the big advantage of using the SR is that the spectra may be taken in minutes.

Our results were collected in the BESSY/Berlin electron storage ring which is one of the brightest synchrotron radiation sources in the X-ray and ultraviolet region from 0.8 nm to about 15 nm. The perspective schematic view of the BESSY storage ring and the optical layout of KMC crystal monochromator beam line [6] together with the schematic for XRA measurement by TYE method are shown in Fig. 2.

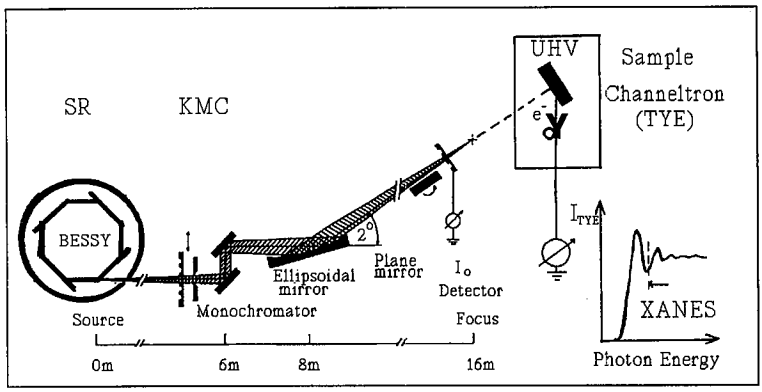

Fig. 2. Schematic for X-ray absorption experiment using synchrotron radiation (SR) from the BESSY/Berlin source with the KMC double crystal monochromator beam line, the total yield electron (TYE) detection in ultra high vacuum chamber (UHV) and schematic XANES spectrum.

We focus our attention only on two experimental aspects of the XANES experiment using SR; the first is the limitation of energy resolution using SR and the second is the TYE technique to record the XRA spectra.

The energy resolution $\Delta E/E$ of the photon beam monochromatized by Bragg diffraction on a crystal monochromator is determined by the angular divergence of the photon beam $\Delta\theta$ ($\Delta E/E = \Delta\theta/\tan\theta$), which is determined by the energy dependent intrinsic vertical spread of the SR and by the source size, i.e. the diameter of the electron beam and its divergence at the emission point. This, in turn, is determined by the electron optics of the storage ring. The resolution depends obviously on the order of harmonics present in the beam and the higher harmonics content [1]. Order sorting monochromators use two crystals and harmonic reduction is achieved when the second crystal is adjusted slightly out of parallel with respect to the first crystal. In such a position it will selectively filter out high-order reflections.

Our Cu L XRA spectra of HTS were collected mainly with the KMC double Crystal Monochromator beam line using beryl [1010] crystals, see Fig. 2, because the photon energy range available with this monochromator due to the beryl lattice constant is limited from 800 eV to about 1550 eV and the copper $L_{II,III}$-edges are

located at about 930 eV. The oxygen K_{I} spectra at about 530 eV were taken with the High-Energy-Plane Grating Monochromator (HE-PGM) with 500 lines/mm of the SX-700 Zeiss type, because it covers the photon energy range from 10 eV to 1400 eV [7]. The energy resolution for the KMC double beryl monochromator was 10^{-3} and was determined mostly by the harmonic contamination of the monochromator, and for the HE-PGM grating monochromator was 5×10^{-4} and most likely was determined by the angular divergence of the photon beam $\Delta\theta$ because $\Delta E/E = \Delta\theta \cot\theta = 2 \times 10^{-4}$.

Both the XANES spectra of copper and of oxygen were recorded by the total yield electron (TYE) technique (see Fig. 2). The TYE mode is normally used because it is sensitive to bulk electronic properties, not the surface ones, and the estimated penetration depth is about 200 Å [8]. This is especially important for ceramic HTS and even single crystals of HTS of which surface may be easily degraded as far as oxygen content and some moisture contaminations are concerned. The $1s$ or $2p$ core level holes, left behind after a X-ray photon absorption process, are filled by electrons from the upper levels and conduction band and the Auger electrons together with normal core photoelectrons are ejected from the sample, as well as causing a shower of inelastic secondary electrons. These yield electrons are detected by channeltron, see Fig. 2. The TYE detection method is competitive to the classical absorption coefficient measurements via the transmission method. The yield electron intensity is always proportional to the absorption coefficient and the equivalency between the transmission and the TYE techniques of XRA measurements was proved both theoretically and experimentally [9]. At high enough photon energies, where reflectivity can be neglected, the yield coefficient $Y(h\omega)$ is proportional to the number of photons absorbed in a layer of an average depth L, namely to $\mu(\omega)L$, where $\mu(\omega)$ is the absorption coefficient. It was argued [9] that the smoothly varying multiplication factor $F(\omega) \propto h\omega$ has to be introduced since the number of created electrons should be proportional to the energy initially deposited in the material. Thus one obtains $Y(\omega) \propto F(\omega)\mu(\omega)L$ and all structure, which occurs in $Y(\omega)$, originates from $\mu(\omega)$. An average depth L which contributes to the yield is typically in order of 30 to 50 Å for metals and about one order of magnitude larger for insulators. That is why one can state that TYE technique is more sensitive for the bulk than the surface.

Our spectra were collected up to the XANES region because we were interested first of all in an electronic structure of unoccupied states around the Fermi level. In fact, the TYE technique both at the Cu L_{III}- and O K_{I}-edges have turned out to be well suited in the investigation of electronic states of Cu and O of the ceramic HTS's.

As the first example, Fig. 3a presents the typical Cu L_{III} XANES spectra of well characterised ceramic $YBa_2Cu_3O_x$ specimens with the chemically determined oxygen content x [10]. For large values of $x \geq 6.3$ these ceramics are the high-temperature superconductors.

In this selective absorption process while a photon of SR is absorbed, the empty states in Cu-$3d$ shell or band are filled by promoting an electron from filled copper $2p$ core level states. This is the Cu L-edge at about 930 eV [11]. In the Cu XANES spectrum there is the so-called "metallic white line" A at

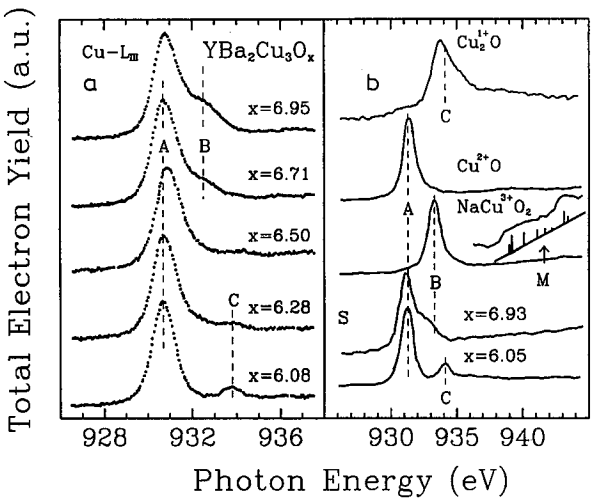

Fig. 3. The copper Cu L_{III} XANES spectra (a) of $YBa_2Cu_3O_x$ with oxygen content x specified and (b) of reference compound Cu_2O, CuO and $NaCuO_2$ in comparison to the superconducting S for $x = 6.93$ and nonsuperconducting for $x = 6.05$ specimens. For the A, B, and C satellites see the text.

$E = 931$ eV, which is typical at the L-edge ($2p$ to $3d$ transition) of transition metals. This line has a large intensity due to the atomic-like character of the d resonace and if the unoccupied final nd states have a narrow bandwidth of 0.2–0.4 eV, the white line maximum corresponds to the Fermi energy E_F. It means that in some cases of covalent systems, multiple-scattering contributions build up bonding and antibonding directional states quite strongly localized. This white line mostly comes from Cu^{2+} ionic state [12] because the main peak A in the XANES spectrum coincides with the white line A for the CuO reference oxide. This is shown in Fig. 3b. In addition to the white line there is also the pronounced satellite B at a slightly higher energy of about 2 eV, of which intensity scales with superconducting transition temperature and vanishes when superconductivity disappears for smaller oxygen content than $x \cong 6.25$. This satellite is connected with physical origin of superconductivity in HTS [12, 13]. Figure 3b shows that coincidence of this peak with the dominant XANES absorption peak of $NaCuO_2$, tetravalent reference compound of copper ionic state, suggests $3d^8$ ground state of copper. But, the signals coming from the $3d^8$ ground state exhibits the typical $2p^53d^9$ final state multiplet structure M [10], indicated by the bar diagrams in Fig. 3b, which is not detected for $YBaCuO_x$ compounds. That is why it has been established that the shoulder B is caused by "formally" tetravalent Cu^{3+} ground state with electronic structure $3d^9L$, which is equivalent to covalent state of Cu^{+2}-$3d^9$ with oxygen ligand hole L (O^{-1} state). This peak assignment is supported in addition by a comparison with the $2p$-core X-ray photoemission spectroscopy [14, 15]. Finally, the XANES peak C, as energetically coincidizing with XANES maximum of Cu_2O

oxide, has been assigned to the Cu^{+1} valency with $3d^{10}$ electronic structure (c.f. Fig. 3b). The same or very similar results have been already observed by a number of authors [16, 17] also for the single crystals.

In order to look directly at the oxygen holes the normalized TYE intensity of Y and Eu samples as a function of incident X-ray photon energy at the O K_I-edges has been measured. It is shown in Fig. 4a. If the holes at the Fermi level in O-$2p$ band due to O^{-1}-$2p^5$ electronic state are filled by promoting an electron from a filled oxygen $1s$ core level state, a selective absorption structure should be seen before the O K_I-edge at about 530 eV [11]. This is really the case as seen from

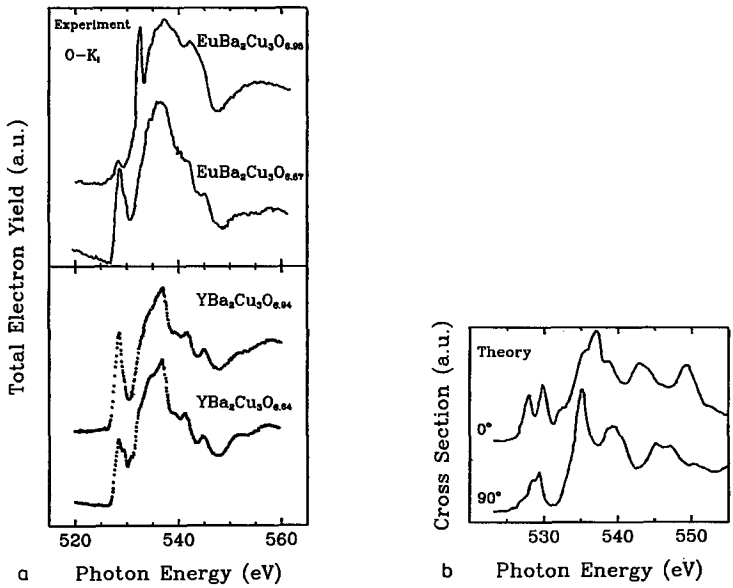

Fig. 4. The oxygen O-K_I XANES spectra: (a) from experiment for the Eu and Y high-temperature superconductors, and (b) calculated, if the angle between the electric field of incident photon beam and c-axis of $YBa_2Cu_3O_x$ crystal is 0° and 90° [16].

the peak in the "low-energy XANES" spectrum in Fig. 4a. The pre-edge peak at about 529 eV, sometimes with double-peaked structure as for Eu specimen, and typical oxygen-edge with pronounced XANES structure above 530 eV are nicely observed. The pre-edge peaks are connected with the $2p^5$ hole final state of O^{-1} ionic state or holes in $2p$ oxygen band. This statement was also proved in other experiments [14–17] and in comparison with theoretical calculations in Fig. 4b [16, 18]. The measurements and calculation for single crystals [16] suggest that there exist oxygen holes of σ-symmetry on all Cu–O bonds. The orientation of the O-$2p$ hole states has been determined from the polarization dependence of the absorption and optical dipole selection rules (c.f. Fig. 4b). With the electric field vector of SR parallel to the a-axis only transitions into p_x orbitals are allowed from an s level, and likewise for the other directions. The O(4) and O(1) holes

are affected the most when oxygen is lost and superconductivity disappears. The holes O(2) and O(3) in the Cu–O_2 planes remain unperturbed. These holes, when pairing, are responsible for superconductivity in HTS materials.

4. Conclusions

The conclusions are twofold:

1) It has been shown that the XANES experiments using the synchrotron radiation are perfectly suitable for getting some crucial information on electronic structure of the high-temperature superconductors.

2) The XANES spectra around the Cu L_{III}- and O K_I-edges demonstrate directly the existence of Cu-$3d^9L$ electronic ground state of formally tetravalent copper ion as well as of unoccupied O-$2p$ state (hole), i.e. O^{-1} electronic state, which are responsible for superconductivity of high-temperature superconductors.

Acknowledgment

I thank Dr. Z. Kąkol for a helping hand in computer elaboration of the drawings.

References

[1] A. Bianconi, in: *X-Ray Absorption; Principles, Applications, Techniques of EXAFS, SEXAFS and XANES*, Eds. D.C. Koningsberger, R. Prins, *Chemical Analysis*: a series of monographs on *Analytical Chemistry and its Applications*, Vol. 92, Wiley Interscience Publication, New York, Toronto, Singapore 1986, p. 573.

[2] P.J. Durham, in Ref. [1], p. 53.

[3] C.R. Natoli, M. Benfatto, *J. Phys. Colloq.* **C8, suppl. 12**, 11 (1986).

[4] E.A. Stern, in Ref. [1], p. 3.

[5] G.S. Brown, S. Doniach, in: *Synchrotron Radiation Research*, Eds. H. Winick, S. Doniach, Plenum Press, New York 1980, p. 353.

[6] J. Feldhaus, F. Schafers, W. Peatman, BESSY Annual Report 1986, p. 314.

[7] H. Petersen, A. Savci, R. Unwin, BESSY Annual Report 1986, p. 314.

[8] G. Martens, P. Rabe, G. Tolkiehn, A. Werner, *Phys. Status Solidi A* **55**, 105 (1979); *J. Phys. C* **11**, 3125 (1978); A. Bianconi, *Appl. Surf. Phys.* **6**, 392 (1980).

[9] C. Kunz, in: *Synchrotron Radiation*, Ed. C. Kunz, *Topics in Current Physics*, Vol. 10, Springer Verlag, Berlin 1979, p. 299.

[10] O. Strebel, G. Kaindl, A. Kołodziejczyk, W. Schafer, R. Kiemel, S. Losch, S. Kemmler-Sack, *J. Mag. Mag. Mater.* **76-77**, 597 (1988).

[11] *Table of Core-Level Binding Energies*, Appendix in: *Synchrotron Radiation*, Ed. C. Kunz, *Topics in Current Physics*, Vol. 10, Springer Verlag, Berlin 1979, p. 299.

[12] G. Kaindl, O. Strebel, A. Kołodziejczyk, W. Schafer, R. Kiemel, S. Losch, S. Kemmler-Sack, R. Hoppe, H.P. Muller, D. Kissel, *Physica B* **158**, 446 (1989).

[13] O. Strebel, P. Sladeczek, M. Asensio, C. Laubschat, A. Kołodziejczyk, R. Miranada, G. Kaindl, *Physica C* **162-164**, 1331 (1990).

[14] P. Steiner, S. Hûfner, A. Jungman, V. Kinsinger, I. Sander, *Z. Phys. B* **74**, 173 (1989).

[15] B.K. Chakraverty, D.D. Sarma, C.N.R. Rao, *Physica C* **156**, 413 (1988).

[16] E.E. Alp, J.C. Campuzano, G. Jennings, J. Guo, D.E. Ellis, L. Beaulaigue, S. Mini, M. Faiz, Y. Zhou, B.W. Veal, J.Z. Liu, *Phys. Rev. B* **40**, 9385 (1989).

[17] R. Nücker, J. Fink, J.C Fuggle, P.J. Durham, W.M. Temmerman, *Phys. Rev. B* **37**, 5158 (1988).

[18] J. Zaanen, A.T. Paxton, O. Jepsen, O.K. Andersen, *Phys. Rev. Lett.* **60**, 2685 (1988); J. Zaanen, O. Jepsen, O. Gunnarsson, A.T. Paxton, O.K. Andersen, *Physica C* **153-155**, 1636 (1988).